Addition Reactions of Alkyl and Carboxyl Radicals to Vinylidene Fluoride

P. Hirunsit and P. B. Balbuena*

Department of Chemical Engineering, Texas A&M University, College Station, Texas 77843

Received: November 21, 2007; Revised Manuscript Received: February 26, 2008

The addition reactions of alkyl radicals CF_3• and CH_3• and carboxyl radicals C_2H_5O•, C_2H_5OCOO•, CF_3COO•, and CH_3COO• to a vinylidene fluoride (VDF) molecule are studied using ab initio calculations. These radicals were selected because they are intermediate or final products of diacyl peroxides decomposition in the initiation reactions of VDF polymerization. Two combinations of methods for energetics and structure optimization are applied: QCISD/6–311G(d,p)//HF/6-31G(d) and B3LYP/6–311G+(3df, 2p)//B3LYP/6–31G(d). It is found that the formed bond length of the product, the forming bond length of the transition state, and the attack angle of the product structures are not sensitive to the level of theory even though the attack angle of the transition state structures is. Early transition states are obtained upon attack at both high-substituted and nonsubstituted carbon atom VDF ends. Kinetic and thermodynamic control rules play different roles on governing the reactivity of the addition with the studied radicals. Both theoretical methods yield the same trends for the preferential attack site in terms of regioselectivity, barrier energies, and reaction enthalpies. It is shown that the addition reactions of the intermediate radicals C_2H_5OCOO•, CF_3COO•, and CH_3COO• of the decomposition of diethyl peroxydicarbonate, trifluoroacetyl peroxide, and diacetyl peroxide initiators yield smaller energy barriers than the additions of the corresponding final radicals, C_2H_5O•, CF_3•, and CH_3•; therefore, the reactions of the intermediate radicals should not be ignored when analyzing the initiation process of the VDF polymerization using those initiators.

1. Introduction

Poly vinylidene fluoride (PVDF) is an important fluoropolymer that presents a unique combination of good mechanical properties, excellent chemical resistance, high thermal stability, and superior resistance to wear, high temperature, corrosion, and weather and possesses good electric insulation and high dielectric constant properties.[1] Also, it is an anti-ultraviolet ray, anti-radiation, and low flammability compound.[1] PVDF is widely used as insulation material for wires, cables, tubing, piping, sheet, and melt-cast films in electronic/electric and computer industries.[1,2] Moreover, it is used in fluid-handling systems for solid and lined pipes, fitting, valves, and pumps in chemical industry.[1,2] Commercial PVDF is usually produced by free radical emulsion and suspension polymerization.[2–5] These polymerization processes involve a free radical polymerization where an initiator generates primary radicals and culminates in addition to the carbon−carbon double bond of a monomer so as to form initiating radicals which continue to the propagation reactions. Vinylidene fluoride is a monomer used to produce PVDF. The radical addition to alkenes is the central reaction in many polymer processes, and it has been studied extensively both experimentally[6–11] and theoretically.[10,12–18] Although extensive and useful experimental information has been reported on the radical addition, theoretical investigations are very useful in offering greater insights into the mechanism, complete geometries and vibrational frequencies of all species can be obtained including transition state structures which are difficult to be determined experimentally. Wong et al.[13] performed a theoretical study of the controlling factors of the addition of methyl radical to monosubstituted alkenes (reaction 1).

$$CH_3\bullet + CH_2{=}CHX \rightarrow CH_3CH_2CHX\bullet \qquad (1)$$

They found that the barrier to this process was primarily governed by reaction thermodynamics whereas polar effects play an unexpectedly small role. This is in contrast to the CH_2OH• radical, which generally exhibits nucleophilic behavior, and to the CH_2CN• radical, which normally shows electrophilic behavior; the reactivities of these radicals are strongly influenced by polar effects. Also, many studies have led to the conclusion that polar, steric, and reaction thermodynamics effects all play a key role in governing reactivity in the radical addition to alkenes.[10,13,19]

One of the important factors that influence the quality of an ab initio calculation is the careful selection of the applied level of theory. Because high quality calculations are usually more expensive, it is necessary to compromise between the accuracy of the estimations and the computational expense. Wong and Radom[12] used various levels of theory in ab initio calculations to study geometry optimization, vibrational frequency analysis, and energetics of the addition of radicals to alkenes where the radicals are CH_3•, CH_2OH•, and CH_2CN•. The results suggested that the use of energies, corrected for zero-point energy (ZPE), given from QCISD/6–31G(d) or B3-LYP/6-31G(d) calculations are preferable to combinations such as UHF/6-31G(d) or UMP2/6-31G(d). Also, energies from B3-LYP/6–311+G(3df,2p) level with B3-LYP/6–31G(d) geometries and ZPE corrections yielded barriers in good agreement with experimental values for methyl radical addition in solution. Additional work from Radom and co-workers[10,12,18,20–23] assessed the procedures for calculations on radical addition and on free radical thermochemistry. In addition, Gomez-Balderas et al.[16] reported a comparative assessment of the accuracy of computational procedures for calculating geometries, frequency factors, barriers and reaction enthalpies for methyl radical addition to C=C double and C≡C

* To whom correspondence should be addressed. E-mail: balbuena@tamu.edu

10.1021/jp711101b CCC: $40.75
Published on Web 04/09/2008

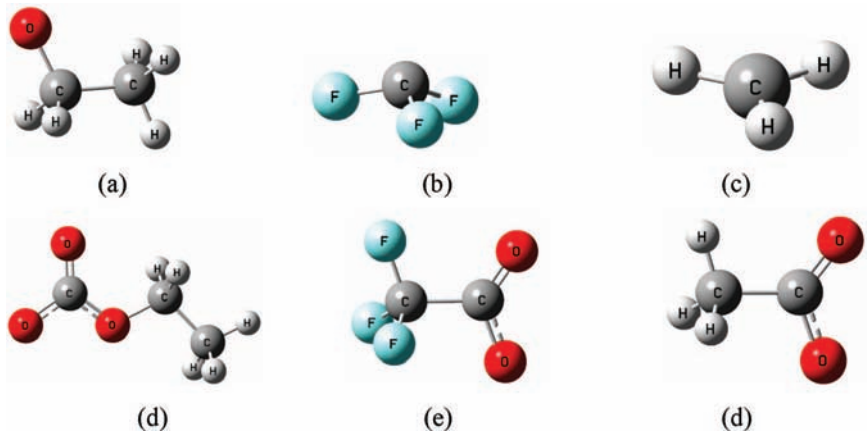

Figure 1. Molecular structures of initiator species: (a) C_2H_5O•, (b) CF_3•, (c) CH_3•, (d) C_2H_5OCOO•, (e) CF_3COO•, and (f) CH_3COO•.

triple using high theoretical levels of the G3-type, W1-type, and CBS-type methods. Furthermore, other properties such as standard enthalpies of formation for a set of hydrocarbons, including alkanes, alkenes, alkynes, and radical molecules ranging from C1−C10 were theoretically studied by Saeys et al.[15] using CBS-QB3 and B3LYP methods. They also reported that the reactivity of carbon-centered radical addition reactions to alkenes of the studied radicals is governed by a combination of polar and reaction thermodynamics factors.

Diacyl peroxides are widely used as radical initiators in free-radical polymerization reactions.[19] Diethyl peroxydicarbonate (DEPDC) is generally used as an initiator in VDF polymerization.[24–26] Peroxydicarbonates are traditionally included in the diacyl peroxide category.[27] Decomposition of diacyl peroxide initiators yields alkyl radicals and may show carboxy radicals as intermediates.[28] In this paper, we use QCISD and B3LYP levels of theory to investigate energy barriers, reaction enthalpies, product and transition state structures of the addition reactions between a VDF monomer and the carboxy radicals (C_2H_5OCOO•, CF_3COO•, CH_3COO•, and C_2H_5O•), and alkyl radicals (CF_3•, and CH_3•) resulting from the decomposition of DEPDC, trifluoroacetyl peroxide (TFAP), and diacetyl peroxide (AP). The decomposition pathways of DEPDC, TFAP, and AP that yield those studied radicals were proposed by Gu et al.[28] Because C_2H_5OCOO•, CF_3COO•, and CH_3COO• are the intermediate radicals during the decompositions of DEPDC, TFAP, and AP, respectively, we are interested in determining if these radical species may favor the addition to VDF better than the final radicals yielded when the decompositions are complete (C_2H_5O•, CF_3•, and CH_3•).

2. Computational Methods

The molecular structures of the studied radicals are shown in Figure 1. The ab initio calculations were performed with the Gaussian03 program[29] for the reactants, products and transition state structures of all species. The addition reactions of the initiator (I•) shown in reactions 2–3 are the result of the asymmetric substitution pattern of VDF.

$$\text{I}\bullet + \text{CH}_2\text{CF}_2 \rightarrow \text{I}-\text{CF}_2-\text{CH}_2\bullet \quad (2)$$

$$\text{I}\bullet + \text{CH}_2\text{CF}_2 \rightarrow \text{I}-\text{CF}_2-\text{CH}_2\bullet \quad (3)$$

where I• are C_2H_5O•, C_2H_5OCOO•, CF_3•, CF_3COO•, CH_3•, and CH_3COO• (Figure 1).

Reaction 2 is head addition, which involves radicals adding to the high-substituted end (CF_2 end) of the double bond, and reaction 3 is tail addition, which involves radicals adding to the nonsubstituted end (CH_2 end) of the double bond.[19]

In a first series of calculations, geometries were optimized and vibrational frequencies and zero-point energies were determined at the UHF/6–31G(d) level. ZPE corrections were calculated from HF/6–31G(d) vibrational frequencies scaled by 0.8929.[12,30] The transition state structures were located using synchronous transit-guided quasi-newton (STQN) methods.[31] Energy barriers and reaction enthalpies were obtained through calculations using the quadratic configuration interaction method, QCISD, with the 6–311G (d,p) basis set. These methods were previously applied to the reaction between the CH_2OH radical and CH_2CCl_2 and the methyl radical with CH_2CCl_2 by Wong and Radom[12] and provided quite good estimations compared to experimental data and other applied theoretical calculation methods. The differences between theory and experiment of energy barrier and reaction enthalpies for the CH_2OH radical were 17 and 6%, respectively.[12] Also, the methyl radical showed differences of 44% for energy barrier and 8% for reaction enthalpy.[12] The energy barrier difference was reduced to 28%[12] when the second series of calculations as described in the next paragraph was applied. Although the calculations with the higher level of theory method, QCISD(T), gave good estimations, the computational expense is quite high, especially with a large system.

In a second series of calculations, we used density functional theory (DFT). Optimized geometries and zero-point energies were obtained at the B3LYP/6–31G(d) level and vibrational frequencies were scaled by 0.9806.[30] Single-point energy calculations were carried out on these optimized structures to determine reaction enthalpies at the B3LYP/6–311G+(3df, 2p) level. This calculation series was also suggested by Wong and Radom,[12] indicating that barriers are usually in good agreement with experiment, with a mean absolute deviation from the experimental values for methyl radical additions in solution of 1.34 kcal/mol where the magnitudes of the experimental barriers are in the range of 3.82–7.27 kcal/mol. Also, this combination has been recommended as the lowest level of theory yielding reasonable reaction barriers and enthalpies.[16] This second method has been chosen because it could be suitable for examining radical additions involving large systems. The results from the two methods are reported for comparative purposes.

The calculated barriers refer to energy differences between transition structures and reactants. Rate coefficients can be obtained with eq 4[32]

$$k(T) = \kappa \frac{k_B T}{\hbar} \frac{Q_{TS}(T)}{Q_{react}(T)} \exp\left(\frac{-\Delta E(0\ \mathrm{K})}{RT}\right) \quad (4)$$

where κ is a transmission coefficient, k_B is the Boltzmann constant, and $\hbar$ is Planck's constant. $Q_x(T)$ stands for the partition functions evaluated at temperature T, and $\Delta E(0\ \mathrm{K})$ is the 0 K energy difference between reactants and transition state, including the zero-point energy difference. The transmission coefficient represents the extent of recrossing where molecules are reflected back to the reactant side and tunneling effect where species with low energy tunnel through the barrier to the product side.[32] For computation of accurate rate coefficients, determination of the transmission coefficient and partition functions with particular attention to internal rotations are required.[16,23,33] However, because the main objective of this paper is to obtain *relative* reactivity trends rather than numerical accuracy of the barriers, the transmission coefficient is assumed to be one, the tunneling correction is not included, and we do not account for hindered internal rotations in the calculation of the partition functions. Rate coefficients are employed to estimate the regioselectivity, measured by a ratio between the rate coefficient of reactions 2 and 3, and we do not report absolute rate results. Thus, the calculation methods were chosen based on accuracy of energy barrier prediction rather than on that of absolute rate coefficients.

3. Results and Discussion

3.1. Geometries. Figure 2 shows schematic molecular structures of the possible formed products. The optimized products resulting from head addition (reaction 2) of the C_2H_5O•, C_2H_5OCOO•, CH_3•, CH_3COO•, and CF_3COO• radicals are more stable than those of tail addition (reaction 3), except for the CF_3• radical whose products from tail addition have lower energy than those from head addition as shown in Table 1. For each radical, the new formed bonds (B1) of the more stable (lowest energy) products are shorter. However, the trend of attacking angles A1 in product structures is not predictable based on product energies. Since the F atoms are strong electron-withdrawing substituents of the alkene, the studied radicals except CF_3• tend to be nucleophilic, even the CH_3• radical which generally prefers to be an electron acceptor rather than an electron donor[10] and this could lead to head addition being a major pathway for the addition of the studied radicals to VDF except for the reactions involving the CF_3• radical. However, in a later section we revise this preliminary conclusion taking into account also energy barriers, reaction enthalpies, and regioselectivity.

The bond lengths B1 of the optimized product structures at the HF/6-31G(d) level of calculation are only slightly shorter (differences of 0.004–0.036 Å) than those given by the B3LYP/6–31G(d) level. The differences in attacking angles A1 between the two methods are in the range of 0.03–1.6°, in agreement with ref 10, which found the attacking angle not particularly sensitive to the level of theory. The formed bond length B1 of the stable products from addition of the following radicals is in the order (from the shortest to the longest): C_2H_5O•, CH_3COO•, C_2H_5OCOO•, CF_3COO•, CF_3•, and CH_3•; thus, as expected, the formed C−O bonds are shorter than the formed C−C bonds. The C−O bonds formed with the C_2H_5O• radical are the strongest compared to C−O bonds formed with the other radicals, and the C−C bonds formed with CF_3• are shorter than those with CH_3•. Although the largest difference of the formed bond from those radicals is only 0.164 Å, a large difference in energy barriers of the reactions is found, as discussed in a later section.

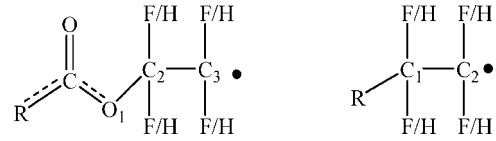

Figure 2. Schematic molecular structures of products, where R represents C_2H_5O, CF_3, and CH_3.

Table 2 lists the calculated forming bond lengths and angles of attack of the transition state structures shown in Figure 3 and their energies. Transition states of CF_3COO• and CH_3COO• radicals could not be located via the DFT method. The energy properties of C_2H_5OCOO• radical at the level of QCISD theory (method 1) could not be reached due to the very high computational expense requirement.

Like in the product structures, the forming bond lengths of the transition state structures calculated at the HF/6–31G(d) level of theory are shorter than those given at B3LYP/6–31G(d) level, with differences in the range 0.013–0.138 Å. The angle of attack differences between the two methods lie between 1.2 and 13.2°. Thus, calculations at the HF/6–31G(d) level and the B3LYP/6–31G(d) level show a very small dependence on the calculation method for the forming bond length but a larger effect on the attack angle in the transition structures for the studied radicals. Unlike the product structures, the angles of attack are more sensitive to the levels of theory. For the given carboxyl radicals, the forming bond length in the transition state structures (Table 2) is longer when the radicals attack the high-substituted carbon atom whereas this trend is the other way around for the products (Table 1). Also, CF_3• but not CH_3• radicals show longer forming bond length of the transition structures of radicals attacking the high-substituted end atom (Table 2).

The energies and geometries of all the transition states (Figure 3 and Tables 2 and 3) more closely resemble the reactants than the products. Considering the results given by DFT (method 2), the lengths of the forming bonds in transition structures are long (more than ∼2.1 Å) and the bond lengths between two carbon atoms in the VDF fragment of the transition structures are much closer to the reactant than to the product ones as shown in Table 3. These results quite clearly show that early transition states are obtained upon attack at both high-substituted and nonsubstituted carbon atoms of a VDF. An early transition state necessarily implies a loose structure with little bond formation and little change in the alkene and radical geometries.[34] Furthermore, in all transition structures, the imaginary frequency is predominantly the radical-VDF C−C stretch. Larger frequencies always correspond to the radical attack at the high-substituted end of VDF except for the C_2H_5O• radical. However, the difference between those frequencies for the C_2H_5O• radical is very small ($-344\ \mathrm{cm}^{-1}$ for attacking the high-substituted end and $-350\ \mathrm{cm}^{-1}$ for attacking the nonsubstituted end).

3.2. Energy Barriers, Reaction Enthalpies, and Regioselectivity. All of the addition reactions are strongly exothermic, and the computed value of energy barriers and reaction enthalpies are shown in Table 4. The difference of energy barriers between the two methods is in the range 0.23–2.11 kcal/mol and lays in the range 4.31–9.19 kcal/mol for reaction enthalpies. For the addition of methyl radical to ethene, Fischer and Radom found that the calculated barriers show a massive dependence on the level of theory used but it affects less to the calculated reaction enthalpies.[10] However for our systems, methods 1 and 2 give the opposite trend (larger differences for reaction enthalpies). The experimental energy barrier data of the CF_3• radical reacting with a high-substituted carbon atom

TABLE 1: Calculated Formed Bond Lengths B1 (Å), Attacking Angle A1 (deg), and Energy E + ZPE (Hartrees) of Products

	B1		A1		E + ZPE[c]	
product species	HF	DFT	HF	DFT	method 1	method 2
$C_2H_5OC^*F_2CH_2$[b]	1.348	1.370	115.0	115.4	−430.46881	−431.54418
$C_2H_5OC^*H_2CF_2$[b]	1.391	1.418	113.6	115.2	−430.44444	−431.52344
$C_2H_5OCOOC^*F_2CH_2$[a]	1.388	1.421	115.6	115.5		−620.17379
$C_2H_5OCOOC^*H_2CF_2$[a]	1.409	1.431	106.8	107.2		−620.16300
$CF_3C^*F_2CH_2$[b]	1.529	1.549	114.3	114.3	−613.46740	−614.85616
$CF_3C^*H_2CF_2$[b]	1.509	1.518	113.2	113.1	−613.47170	−614.86263
$CF_3COOC^*F_2CH_2$[a]	1.391	1.425	109.2	108.8	−801.18708	−803.46636
$CF_3COOC^*H_2CF_2$[a]	1.426	1.462	109.9	111.2	−801.17339	−803.45994
$CH_3CF_2C^*H_2$[b]	1.512	1.521	115.6	115.8	−316.21884	−317.00584
$CH_3CH_2C^*F_2$[b]	1.528	1.532	112.6	112.7	−316.21351	−317.00240
$CH_3COOC^*F_2CH_2$[a]	1.378	1.406	109.4	109.1	−504.37906	−505.62362
$CH_3COOC^*H_2CF_2$[a]	1.417	1.450	109.9	111.0	−504.36597	−505.61599

[a] B1 is the bond length between O1 and C2 (Figure 2a). A1 is the angle of O1−C2−C3 (Figure 2a). [b] B1 is the bond length between R and C1 (Figure 2b). A1 is the angle of R−C1−C2 (Figure 2b). [c] Energy values (without ZPE) are listed in Supporting Information. * Indicates attack site.

TABLE 2: Forming Bond Length (Å), Angle of Attack (deg), and Energies + ZPE (hartrees) of the Transition State Structures

		forming bond length			angle of attack			energy + ZPE[b]	
radical reactant	site of attack*	atom[a]	HF	DFT	atom[a]	HF	DFT	method 1	method 2
C_2H_5O•	$^*CF_2{=}CH_2$	2-14	1.952	2.080	1-2-14	103.5	93.8	−430.40767	−431.49624
	$CF_2{=}C^*H_2$	1-14	1.908	2.047	2-1-14	110.7	103.5	−430.40481	−431.49426
C_2H_5OCOO•	$^*CF_2{=}CH_2$	7-1	2.071	2.190	8-7-1	99.2	86.0		−620.13470
	$CF_2{=}C^*H_2$	14-1	2.014	2.807	13-14-1	103.2	79.1		−620.13591
CF_3•	$^*CF_2{=}CH_2$	2-1	2.258	2.382	3-2-1	103.4	101.81	−613.40473	−614.80928
	$CF_2{=}C^*H_2$	3-1	2.244	2.271	2-3-1	109.5	106.6	−613.40834	−614.81396
CF_3COO•	$^*CF_2{=}CH_2$	5-1	2.190		6-5-1	91.5		−801.12810	
	$CF_2{=}C^*H_2$	6-1	2.077		5-6-1	104.9		−801.13805	
CH_3•	$^*CF_2{=}CH_2$	2-1	2.259	2.281	3-2-1	106.4	103.9	−316.16057	−316.94944
	$CF_2{=}C^*H_2$	3-1	2.283	2.345	2-3-1	109.9	111.1	−316.16265	−316.95290
CH_3COO•	$^*CF_2{=}CH_2$	5-1	2.111		6-5-1	94.6		−504.31689	
	$CF_2{=}C^*H_2$	6-1	1.999		5-6-1	106.6		−504.32938	

[a] Atom numbers refer to Figure 3. [b] Energy values (without ZPE) are listed in Supporting Information.

is 5.2 kcal/mol;[35] thus, from the results in Table 4, the calculated barriers using methods 1 and 2 are 1.87 and 1.11 kcal/mol higher than this experimental value, respectively. The experimental barrier energy of CF_3• attacking the nonsubstituted carbon atom is 3.2 kcal/mol,[35] and the theoretical results using methods 1 and 2 overestimate this value by 1.6 and 0.17 kcal/mol, respectively. The experimental trend yielding higher energy barrier for the head than for the tail CF_3• addition is followed by the calculated barriers. On the other hand, the experimental barrier energies of CH_3• radical addition to the non-fluorinated carbon atom is 11.2 kcal/mol[11] whereas methods 1 and 2 slightly underestimate the barriers, yielding 10.8 and 8.69 kcal/mol, respectively, and the experimental barrier for addition of CH_3• to the fluorinated carbon atom has been reported to be 8.2 kcal/mol[11] that is overestimated by methods 1 and 2 predictions of 12.1 and 10.86 kcal/mol, respectively. In this case, none of the methods follow the experimental trend that yields lower barrier to the head addition.

The regioselectivity is another indicator of which end of a substrate is preferentially attacked by a radical as measured by the ratio between the rate coefficient of the addition attacking the carbon atom at the CF_2 end and that at the CH_2 end. Table 5 shows that the regioselectivity trends are the same for both methods, suggesting preferential tail attack except for C_2H_5O• and CF_3COO•, which show preferential head attack. Also, the same trends suggested by the regioselectivity analysis is indicated by the calculated energy barriers (Table 4, except for the addition of CF_3COO• radical) suggesting that the radicals have more propensities to attack at the end of VDF, which gives lower energy barriers. The experimental regioselectivity ratio of the addition of CF_3• radical to VDF at the CF_2 end and at the CH_2 end is 0.03:1 at 423 K[11] and that of the CH_3• radical is 0.179:1[35] at the same temperature, in qualitative agreement with the calculated values listed in Table 5. To the best of our knowledge, experimental thermodynamic data for the additions of C_2H_5O•, C_2H_5OCOO•, CF_3COO•, and CH_3COO• to VDF have not been reported.

Experimental work on the radical CH_3• addition reported that the ratio of attack at the non-fluorinated substituted end of VDF is about six times greater than the attack at the more substituted end at 423 K.[11] This large propensity of the CH_3• radicals to react with the non-fluorinated carbon atom of VDF is confirmed by the theoretical results. As shown in Table 4, the addition reaction of a CH_3• radical to the less-substituted attack site of VDF is characterized by a lower barrier height (8.69 kcal/mol) and the regioselectivity (Table 5) is 0.188:1 (obtained by method 1) between the attack at the CF_2 end and at the CH_2 end. Also, the forming bonds in transition structures of the addition reaction of a CH_3• radical to the nonsubstituted attack site are longer. Regarding reaction enthalpies, the addition to the nonsubstituted end gives lower reaction enthalpy (−23.71 kcal/mol) only slightly different than −25.58 kcal/mol for the addition to the fluorinated end. This may confirm a large predominance of the steric control rule, the preferential attack should occur to the non substituted carbon atom,[34] whereas the thermodynamic control rule that the most exothermic reaction should be the easiest[34] is not followed.

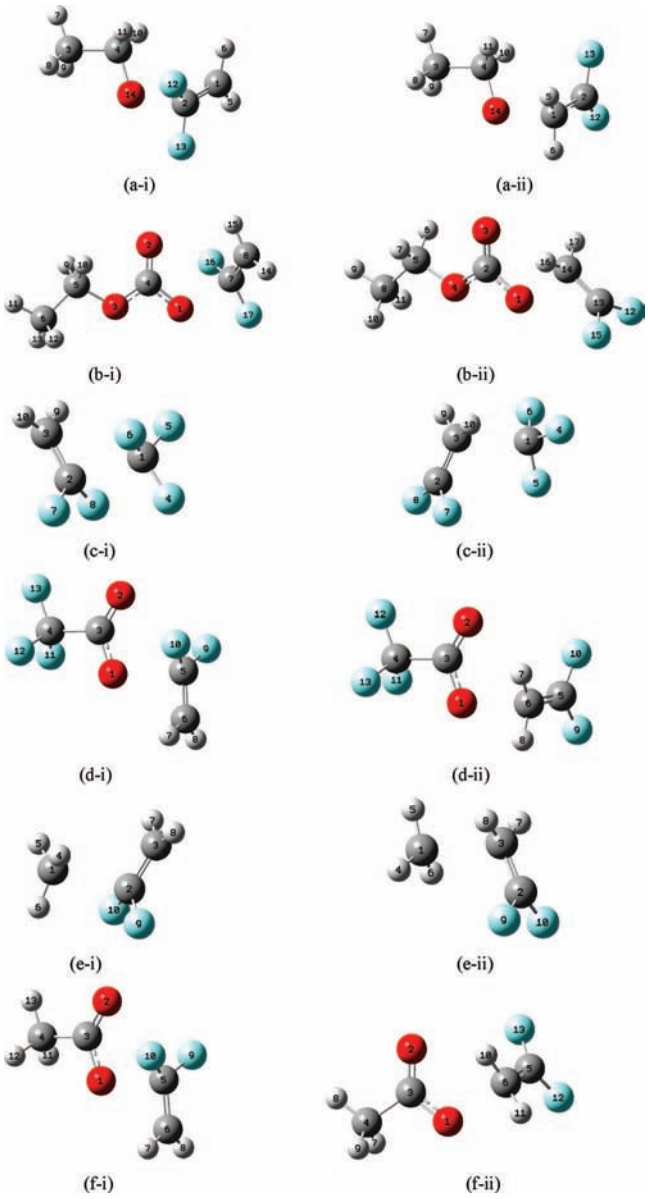

Figure 3. Transition structures of the addition reactions between VDF monomer and radicals (a) C_2H_5O•, (b) C_2H_5OCOO•, (c) CF_3•, (d) CF_3COO•, (e) CH_3•, and (f) CH_3COO•. (x-i) is the radical reacting with the fluorinated carbon atom and (x-ii) is the radical reacting with the non-fluorinated carbon atom.

Experiments on the addition reaction of the CF_3• radical to VDF show that at 423 K the attack at the nonsubstituted end of VDF is 33 times higher than at the more substituted end,[11] in qualitative agreement with the results of both methods shown in Table 5. According to method 2, the energy barrier corresponding to the attack at the nonsubstituted carbon atom is ~2.94 kcal/mol lower than that corresponding to the attack at the more substituted carbon atom. Also, the reaction enthalpies favor the attack at the nonsubstituted carbon atom. Therefore, the calculations suggest that the addition of CF_3• to VDF is either kinetically or thermodynamically favored whereas the addition of CH_3• to the nonsubstituted end of VDF is kinetically favored.

The addition of the CF_3COO• radical to the VDF nonsubstituted carbon atom gives lower barrier energy than that at the other end, whereas the regioselectivity and the reaction enthalpies yield the opposite trend, favoring the attack at the fluorinated end. In this case, the barriers and regioselectivity lead to a different preferential attack site; however, the barriers of both attack sites differ only by 0.13 kcal/mol; such small difference is not enough to show that the CH_2 end is preferred. Also, the regioselectivity trends tend to be more reliable than the absolute results of energy barriers yielding better agreement of the preferential attack site with the experimental results as discussed earlier. It is interesting to point out that the addition of CF_3COO• to VDF at either end shows much lower energy barriers (78 times lower for the attack at the CH_2 end and 37 times lower for the attack at the CF_2 end) than those of the addition of the CF_3• radical. Thus, the CF_3COO• radical could be more reactive, and its addition to VDF during the decomposition of TFAP can not be overlooked in the initiation step of the free radical polymerization of PVDF using TFAP as an initiator. However, temperature and solvent factors have not been addressed in this analysis except for the temperature effects implicit in the regioselectivity analysis.

The radical CH_3COO• is an intermediate of the decomposition of the AP initiator. Considering the results obtained from method 1, the radical CH_3COO• yields lower energy barriers than those of the CH_3• radical for either the attacks at the fluorinated or at the non-fluorinated carbon atom of VDF, especially the addition at the non-fluorinated carbon atom is about 31 times lower. Thus, the addition to CH_3COO• should not be disregarded when the initiator AP is considered. Also, the regioselectivity analysis (Table 5) and the energy barriers (Table 4) show that CH_3COO• greatly prefers to attack the nonsubstituted end of VDF. Thus, like the CH_3• radical, although reaction enthalpies favor the attack at the high-substituted end the kinetic results (barriers and regioselectivity) suggest that the addition will be at the nonsubstituted end. Furthermore, CH_3• and CH_3COO• radicals are nucleophilic and they still add preferentially to the nonsubstituted end of VDF, confirming that the steric effect may become more important than the polarity influence for these addition reactions.

DEPDC is the typical initiator used for VDF polymerization. As shown in Table 4, the C_2H_5O• radical does not yield significant lower barrier energies or higher exothermicities compared to the other studied radicals. Based on the lower energy barrier, larger exothermicity (Table 4), and regioselectivity ratio (Table 5), the radical C_2H_5O• kinetically and thermodynamically preferentially adds to the fluorinated carbon atom of VDF. The higher energy barriers of the addition correspond to shorter forming bond lengths in the transition structures for both C_2H_5O• and C_2H_5OCOO• radicals. Considering the polarity influence, the C_2H_5O• radicals are nucleophilic and they likely add preferentially to the substituted end of VDF. This clearly suggests that the polar effect is more dominant than the steric effect for the addition of C_2H_5O• to VDF. On the other hand, according to barrier heights and regioselectivity, the intermediate radical C_2H_5OCOO• generated by the DEPDC decomposition preferentially adds to the nonsubstituted end, and it has lower barrier heights than the radical C_2H_5O• on either attack sites. Therefore, the addition reaction of C_2H_5OCOO• to VDF should not be overlooked in the analysis of DEPDC initiated VDF polymerization. However, this study does not consider the effect caused by other factors such as temperature (except that included in the regioselectivity analysis) which may be important for the initiation process.

4. Conclusions

The addition reactions of alkyl radicals CF_3• and CH_3• and carboxyl radicals C_2H_5O•, C_2H_5OCOO•, CF_3COO•, and CH_3COO• to VDF are studied using ab initio calculations to

TABLE 3: C−C Bond Lengths (Å) of VDF Fragment in Transition State Structures and Products[a]

		r(C═C) of transition state structures		*r*(C−C) of product structures	
species	attack site	method 1	method 2	method 1	method 2
C_2H_5O•	*CF_2═CH_2	1.378	1.352	1.493	1.489
	CF_2═C*H_2	1.386	1.350	1.450	1.504
C_2H_5OCOO•	*CF_2═CH_2	1.366	1.356	1.486	1.481
	CF_2═C*H_2	1.366	1.331	1.496	1.499
CF_3•	*CF_2═CH_2	1.367	1.351	1.486	1.481
	CF_2═C*H_2	1.359	1.342	1.498	1.501
CF_3COO•	*CF_2═CH_2	1.372		1.484	1.482
	CF_2═C*H_2	1.352		1.493	1.489
CH_3•	*CF_2═CH_2	1.373	1.352	1.491	1.488
	CF_2═C*H_2	1.367	1.346	1.495	1.498
CH_3COO•	*CF_2═CH_2	1.385		1.487	1.485
	CF_2═C*H_2	1.363		1.494	1.492

[a] *r*(C═C) of VDF = 1.304 Å (method 1) and 1.322 Å (method 2).

TABLE 4: Calculated Energy Barriers and Reaction Enthalpies (kcal/mol)

		barrier		enthalpy[a]	
radical reactants	attack site at*	method 1	method 2	method 1	method 2
C_2H_5O•	*CF_2═CH_2	6.69	6.46	−32.14	−23.76
	CF_2═C*H_2	8.48	7.71	−17.04	−10.97
C_2H_5OCOO•	*CF_2═CH_2		3.50		−21.14
	CF_2═C*H_2		2.74		−14.47
CF_3•	*CF_2═CH_2	7.07	6.31	−32.33	−23.14
	CF_2═C*H_2	4.80	3.37	−35.35	−27.59
CF_3COO•	*CF_2═CH_2	0.19		−36.85	
	CF_2═C*H_2	0.06		−28.49	
CH_3•	*CF_2═CH_2	12.10	10.86	−30.85	−25.58
	CF_2═C*H_2	10.80	8.69	−28.02	−23.71
CH_3COO•	*CF_2═CH_2	8.18		−30.98	
	CF_2═C*H_2	0.35		−22.98	

[a] At 298 K.

TABLE 5: Calculated Regioselectivity Defined As a Ratio between the Rate Coefficient of the Addition Attacking at the Carbon Atom of High-Substituted End (Head) and That of the Nonsubstituted End (Tail)

	CF_2═CH_2	
radical	method 1	method 2
C_2H_5O•	20.216:1[a]	7.533:1[a]
C_2H_5OCOO•		0.004:1[a]
CF_3•	0.03:1[a] 0.093:1[b]	0.013:1[a] 0.056:1[b]
CF_3COO•	2.621:1[a]	
CH_3•	0.098:1[a] 0.188:1[b]	0.012:1[a] 0.035:1[b]
CH_3COO•	$5.06*10^6$:1[a]	

[a] At 298 K. [b] At 423 K.

characterize product and transition structures, energy barriers, reaction enthalpies, and regioselectivity. Two methods are applied: the first consists of reactant, transition and product structure optimizations using UHF/6–31G(d) and energies calculated using QCISD/6–311G(d,p), and the second method involves structure optimization via B3LYP/6-31G(d) whereas B3LYP/6–311G+(3df, 2p) is used for the energetics. The formed bond length of the product, the forming bond length of the transition state, and the attack angle of the product structures are not sensitive to the level of theory but the attack angle of the transition state structures is. The C_2H_5O• radicals make the strongest formed C−O bonds compared to the other studied radicals. Early transition states are obtained upon attack at both high- and nonsubstituted carbon atom ends of VDF.

Both methods yield the same trends for the preferential attack site in terms of regioselectivity, energy barriers and reaction enthalpies. The regioselectivity suggests the same preferential attack location with that given by the energy barriers, except for the CF_3COO• radical. The regioselectivity analysis indicates that attacks at the high-substituted carbon atom end of VDF for C_2H_5O• and CF_3COO•, and at the nonsubstituted carbon atom end for the additions of C_2H_5OCOO•, CF_3•, CH_3•, and CH_3COO• radicals are more favorable, whereas analyses of the reaction enthalpies imply the opposite trends for C_2H_5OCOO•, CH_3•, and CH_3COO•. Thus, it is suggested that the addition reaction of C_2H_5OCOO•, CH_3•, and CH_3COO• radicals to VDF is most likely dominated by kinetic than by thermodynamic control rules. For the addition of the CF_3COO• radical, regioselectivity favors addition to the CF2 end, and the same trend is suggested by the reaction enthalpy values but the energy barrier shows preferential addition to the CH2 end, although the energy barrier difference of the two attack sites is so small that we could conclude that both thermodynamics and kinetic factors are dominant for CF_3COO• additions. On the other hand, kinetic and thermodynamic control rules are in agreement for the addition of the CF_3• radical, and also for the addition of the C_2H_5O• radical where the polar effect overrides the steric effect. The carboxyl radicals C_2H_5OCOO• and CH_3COO• show very small tendency adding to the substituted end of VDF (in contrast to CF_3COO•) and they are nucleophilic radicals. Thus, for them, the steric effect overrides the polar effect. The addition reaction of the intermediate radicals C_2H_5OCOO•, CF_3COO•, and CH_3COO• of the decomposition of DEPDC, TFAP, and AP initiators show smaller barrier heights than the addition of the corresponding final radicals: C_2H_5O•, CF_3•, and CH_3•. Thus, the addition reactions of those intermediate radicals should be taken into account when VDF polymerization initiators such as DEPDC, TFAP, or AP are used. However, it should be noted

that this study does not consider solvent and temperature effects which may be significant in the initiation process as well.

Acknowledgment. This work is supported by the National Science Foundation. Discussions with Prof. George Roberts and Prof. Keith Gubbins are gratefully acknowledged. P.H. thanks the National Nanotechnology Center of Thailand for providing a scholarship.

Supporting Information Available: Table containing the absolute energies corresponding to products and transition state structures. This material is available free of charge via the Internet at http://pubs.acs.org.

References and Notes

(1) Scheinbeim, J. *Poly(vinylidene fluoride)*; Oxford University Press: Oxford, 1999.

(2) Charpentier, P. A.; DeSimone, J. M.; Roberts, G. W. Continuous Precipitation Polymerization of Vinylidene Fluoride in Supercritical Carbon Dioxide: Modeling the Rate of Polymerization. *Ind. Eng. Chem. Res.* **2000**, *39*, 4588–4596.

(3) Guiot, J.; Ameduri, B.; Boutevin, B. Radical Homopolymerization of Vinylidene Fluoride Initiated by tert-Butyl Peroxypivalate. Investigation of the Microstructure by ^{19}F and ^{1}H NMR Spectroscopies and Mechanisms. *Macromolecules* **2002**, *35*, 8694–8707.

(4) Apostolo, M.; Arcella, V.; Storti, G.; Morbidelli, M. Kinetics of the Emulsion Polymerization of Vinylidene Fluoride and Hexafluoropropylene. *Macromolecules* **1999**, *32*, 989–1003.

(5) Russo, S.; Behari, K.; Chengji, S.; Pianca, M.; Barchiesi, E.; Moggi, G. Synthesis and microstructural characterization of low-molar-mass poly(vinylidene fluoride). *Polymer* **1993**, *34*, 4777–4781.

(6) Low, H. C.; Tedder, J. M.; Walton, J. C. Free radical addition to olefins. Part 20.—A reinvestigation of the addition of methyl radicals to fluoroethylenes. *J. Chem. Soc., Faraday Trans. 1* **1976**, *72*, 1707–1714.

(7) Zytowski, T.; Fischer, H. Absolute Rate Constants for the Addition of Methyl Radicals to Alkenes in Solution: New Evidence for Polar Interactions. *J. Am. Chem. Soc.* **1996**, *118*, 437–439.

(8) Batchelor, S. N.; Fischer, H. Radical Addition Rates to Alkenes by Time-Resolved CIDNP: 2-Hydroxy-2-propyl Radicals. *J. Phys. Chem.* **1996**, *100*, 9794–9799.

(9) Zytowski, T.; Fischer, H. Absolute Rate Constants and Arrhenius Parameters for the Addition of the Methyl Radical to Unsaturated Compounds: The Methyl Affinities Revisited. *J. Am. Chem. Soc.* **1997**, *119*, 12869–12878.

(10) Fischer, H.; Radom, L. Factors Controlling the Addition of Carbon-Centered Radicals to Alkenes - An Experimental and Theoretical Perspective. *Angewandte Chemie International Edition* **2001**, *40*, 1340–1371.

(11) Tedder, J. M.; Walton, J. C.; Winton, K. D. R. Free radical addition to olefins. Part 9.—Addition of methyl radicals to fluoro-ethylenes. *J. Chem. Soc., Faraday Trans. 1* **1972**, *68*, 1866–1873.

(12) Wong, M. W.; Radom, L. Radical Addition to Alkenes: Further Assessment of Theoretical Procedures. *J. Phys. Chem. A* **1998**, 102.

(13) Wong, M. W.; Pross, A.; Radom, L. Comparison of the Addition of CH_3•, CH_2OH•, and CH_2CN• Radicals to Substituted Alkenes: A Theoretical Study of the Reaction Mechanism. *J. Am. Chem. Soc.* **1994**, *116*, 6284–6292.

(14) R, J; Berry, P. M. A computational study of the reaction kinetics of methyl radicals with trifluorohalomethanes. *Int. J. Chem. Kinet.* **1998**, *30*, 179–184.

(15) Saeys, M.; Reyniers, M. F.; Marin, G. B.; VanSpeybroeck, V.; Waroquier, M. Ab Initio Calculations for Hydrocarbons: Enthalpy of Formation, Transition State Geometry, and Activation Energy for Radical Reactions. *J. Phys. Chem. A* **2003**, *107*, 9147–9159.

(16) Gomez-Balderas, R.; Coote, M. L.; Henry, D. J.; Radom, L. Reliable Theoretical Procedures for Calculating the Rate of Methyl Radical Addition to Carbon-Carbon Double and Triple Bonds. *J. Phys. Chem. A* **2004**, *108*, 2874–2883.

(17) Van Speybroeck, V.; Van Cauter, K.; Coussens, B.; Waroquier, M. Ab Initio Study of Free-Radical Polymerizations: Cost-Effective Methods to Determine the Reaction Rates. *ChemPhysChem* **2005**, *6*, 180–189.

(18) Wong, M. W.; Radom, L. Radical Addition to Alkenes: An Assessment of Theoretical Procedures. *J. Phys. Chem.* **1995**, *99*, 8582–8588.

(19) Moad, G.; Solomon, D. H. *The Chemistry of Free Radical Polymerization*, 1st ed.; Pergamon: Great Britain, 1995.

(20) Smith, B. J.; Radom, L. Heat of Formation of the tert-Butyl Radical. *J. Phys. Chem. A* **1998**, *102*, 10787–10790.

(21) Paul, M. M.; Christopher, J. P.; David, M. S.; Leo, R. An assessment of theoretical procedures for the calculation of reliable free radical thermochemistry: A recommended new procedure. *J. Chem. Phys.* **1998**, *108*, 604–615.

(22) Henry, D. J.; Parkinson, C. J.; Mayer, P. M.; Radom, L. Bond Dissociation Energies and Radical Stabilization Energies Associated with Substituted Methyl Radicals. *J. Phys. Chem. A* **2001**, *105*, 6750–6756.

(23) Heuts, J. P. A.; Gilbert, R. G.; Radom, L. Determination of Arrhenius Parameters for Propagation in Free-Radical Polymerizations: An Assessment of ab Initio Procedures. *J. Phys. Chem.* **1996**, *100*, 18997–19006.

(24) Tai, H.; Wang, W.; Martin, R.; Liu, J.; Lester, E.; Licence, P.; Woods, H. M.; Howdle, S. M. Polymerization of Vinylidene Fluoride in Supercritical Carbon Dioxide: Effects of Poly(dimethylsiloxane) Macromonomer on Molecular Weight and Morphology of Poly(vinylidene fluoride). *Macromolecules* **2005**, *38*, 355–363.

(25) Liu, J.; Tai, H.; Howdle, S. M. Precipitation polymerisation of vinylidene fluoride in supercritical CO2 and real-time calorimetric monitoring. *Polymer* **2005**, *46*, 1467–1472.

(26) Charpentier, P. A.; Kennedy, K. A.; DeSimone, J. M.; Roberts, G. W. Continuous Polymerizations in Supercritical Carbon Dioxide: Chain-Growth Precipitation Polymerizations. *Macromolecules* **1999**, *32*, 5973–5975.

(27) Hiatt, R. *Acyl peroxides*; Wiley: New York, 1970.

(28) Gu, Z.; Wang, Y.; Balbuena, P. B. Does the Decomposition of Peroxydicarbonates and Diacyl Peroxides Proceed in a Stepwise or Concerted Pathway. *J. Phys. Chem. A* **2006**, *110*, 2448–2454.

(29) Frisch, M. J.; Trucks, G. W.; Schlegel, H. B.; Scuseria, G. E.; Robb, M. A.; Cheeseman, J. R.; Montgomery, J. A., Jr.; Vreven, T.; Kudin, K. N.; Burant, J. C.; Millam, J. M.; Iyengar, S. S.; Tomasi, J.; Barone, V.; Mennucci, B.; Cossi, M.; Scalmani, G.; Rega, N.; Petersson, G. A.; Nakatsuji, H.; Hada, M.; Ehara, M.; Toyota, K.; Fukuda, R.; Hasegawa, J.; Ishida, M.; Nakajima, T.; Honda, Y.; Kitao, O.; Nakai, H.; Klene, M.; Li, X.; Knox, J. E.; Hratchian, H. P.; Cross, J. B.; Bakken, V.; Adamo, C.; Jaramillo, J.; Gomperts, R.; Stratmann, R. E.; Yazyev, O.; Austin, A. J.; Cammi, R.; Pomelli, C.; Ochterski, J. W. P.; Ayala, P. Y.; Morokuma, K.; Voth, G. A.; Salvador, P.; Dannenberg, J. J.; Zakrzewski, V. G.; Dapprich, S.; Daniels, A. D.; Strain, M. C.; Farkas, O.; Malick, D. K.; Rabuck, A. D.; Raghavachari, K.; Foresman, J. B.; Ortiz, J. V.; Cui, Q.; Baboul, A. G.; Clifford, S.; Cioslowski, J.; Stefanov, B. B.; Liu, G.; Liashenko, A.; Piskorz, P.; Komaromi, I.; Martin, R. L.; Fox, D. J.; Keith, T.; Al-Laham, M. A.; Peng, C. Y.; Nanayakkara, A.; Challacombe, M.; Gill, P. M. W.; Johnson, B.; Chen, W.; Wong, M. W.; Gonzalez, C.; Pople, J. A. *Gaussian 03*, revision C.02; Gaussian, Inc.: Wallingford, CT, 2004.

(30) Scott, A. P.; Radom, L. Harmonic Vibrational Frequencies: An Evaluation of Hartree-Fock, Moller-Plesset, Quadratic Configuration Interaction, Density Functional Theory, and Semiempirical Scale Factors. *J. Phys. Chem.* **1996**, *100*, 16502–16513.

(31) Peng, C. Y.; Ayala, P. Y.; Schlegel, H. B.; Frisch, M. J. Using redundant internal coordinates to optimize equilibrium geometries and transition states. *J. Comput. Chem.* **1996**, *17*, 49–56.

(32) Eyring, H. The Activated Complex in Chemical Reactions. *J. Chem. Phys.* **1935**, *3*, 107–115.

(33) Van Speybroeck, V.; Van Neck, D.; Waroquier, M.; Wauters, S.; Saeys, M.; Marin, G. B. Ab Initio Study of Radical Addition Reactions: Addition of a Primary Ethylbenzene Radical to Ethene (I). *J. Phys. Chem. A* **2000**, *104*, 10939–10950.

(34) Delbecq, F.; Ilavsky, D.; Nguyen Trong, A.; Lefour, J. M. Theoretical study of regioselectivity in radical additions to substituted alkenes. 1. Hydrogen addition to ethylene, vinylamine, and vinylborane. *J. Am. Chem. Soc.* **1985**, *107*, 1623–1631.

(35) Tedder, J. M.; Walton, J. C. The kinetics and orientation of free-radical addition to olefins. *Acc. Chem. Res.* **1976**, *9*, 183–191.

JP711101B